Optimization of Inlet Temperature for Deactivating LTWGS Reactor Performance

J. L. Ayastuy, M. A. Gutiérrez-Ortiz, J. A. González-Marcos, A. Aranzabal, and J. R. González-Velasco
Group of Chemical Technologies for Environmental Sustainability, Dept. of Chemical Engineering, Faculty of Science and Technology, Universidad del País Vasco/Euskal Herriko Unibertsitatea, 48080 Bilbao, Spain

DOI 10.1002/aic.10433
Published online April 28, 2005 in Wiley InterScience (www.interscience.wiley.com).

An industrial Cu-based low-temperature water-gas shift (LTWGS) reactor, subject to deactivation by irreversible chlorine adsorption, has been modeled and optimized. Both the chlorine adsorption kinetics and deactivation kinetics were assumed first order to chlorine partial pressure, and the rate constants were considered independent of temperature. The Efficient Production (EP) method has been used to compute the reactor production until the outlet CO conversion decays below a permissible minimum level. Two alternative strategies for the inlet temperature have been used to maximize the EP: constant and time-variable. Compared to the EP obtained for the optimum constant inlet temperatures, EP resulting from the use of the optimum time-variable inlet temperature sequence were higher, affording important energy savings. Furthermore, a sensitivity study with respect to most influential operational variables, such as inlet total flow rate, steam-to-gas ratio, pressure, and concentrations of chlorine, hydrogen, carbon monoxide, and inert content, was carried out. © 2005 American Institute of Chemical Engineers *AIChE J,* 51: 2016–2023, 2005
Keywords: LTWGS reaction, poisoning, reactor modeling, optimization, efficient production

Introduction

The water–gas shift reaction (WGSR) is a reversible, exothermic reaction ($\Delta H^0 = -41.1$ kJ/mol)

$$CO + H_2O \leftrightarrows CO_2 + H_2 \quad (1)$$

whose main application focuses on cleaning of CO content and obtaining H_2-rich effluents to be used in ammonia synthesis or PEM (proton-exchange membrane) fuel cells.[1-3]

In industrial operation conditions, when high purity of H_2 is not required, the reaction is carried out in a single bed,[4-6] whereas high-purity hydrogen, as for ammonia production plants, is produced by WGSR carried out in two consecutive adiabatic stages. In the first stage, called high-temperature WGS (HTWGS) reactor, conversion of the carbon monoxide bulk is performed on iron-based catalysts, at elevated temperatures.[7-10] When required, the outlet gases from the HTWGS (containing about 3 vol % of CO) are cooled by adding steam and fed into a second stage, a fixed-bed tubular reactor with copper-based catalyst, called low-temperature WGS (LTWGS) reactor, which operates at moderately low temperatures (453–503 K).[11-14] Because of the exothermicity and equilibrium limitations, in this second stage, the outlet CO concentration is diminished below 0.3 vol %.

However, the main operational problems of Cu-based LTWGS catalyst are its high susceptibility to poisoning, especially to the sulfur and chlorine,[5,15] and its liability to sinter. Sulfur in the feed stream is removed by the use of a guard bed previous to the reactor.[6,15] Chlorine, present in the feed stream from compressor lubrificants or quench water used to control the inlet temperature, irreversibly deactivates the catalyst blocking its sites at typical LTWGSR inlet concentration as low as 10^{-3} ppm.[16-19] Because small crystallites of copper

Correspondence concerning this article should be addressed to J. R. González-Velasco at iqpgovej@lg.ehu.es.

Table 1. Low-Temperature WGS Industrial Reactor Operating Conditions

Variable	Value
P (MPa)	1723
Gas flow rate (mol/h)	1220
Steam/gas	0.61
P_{Cl} (Pa)	6.383×10^{-4}
W (g)	384
$CO/H_2/CO_2/N_2$ (vol %)	3.2/76.8/18.16/1.84

already sinter at temperatures about 503 K, the Cu-based LTWGS catalysts must operate below this temperature.[20]

Because the deactivation of industrial LTWGS catalyst by chlorine occurs within a long period of time (about 2–3 years), the possibility of cyclic regeneration is not feasible and thus an optimum inlet temperature strategy is used to counteract the catalyst deactivation.

In the literature, studies treating the problem of optimization of reactors subject to catalyst decay, either tubular[21-24] or batch reactors,[25-27] as well as isothermal[28,29] or adiabatic[30,31] inclusive of enzymatic reactors,[32] may be found. In this paper, an optimization of the industrial adiabatic plug-flow LTWGS reactor, subject to irreversible poisoning, is presented.

The reduction of CO content in the H_2-rich gas also has economic importance, such as in ammonia plants.[15] Thus, a maximum admissible CO content at the LTWGS reactor outlet has been considered (assuming a minimum permissible CO outlet conversion of 0.85).

In this work, the Cu-based LTWGS industrial reactor subject to deactivation has been modeled and optimized, calculating the reactor inlet temperature policies, constant and time-varying, to maximize the *Efficient Production*. Also, a sensitivity study with respect to operational variables and reactor inlet composition has been carried out.

Reactor Modeling

To model the reactor, typical industrial LTWGS conditions, as listed in Table 1, were taken.[33]

LTWGSR kinetics

We previously described the kinetics of the LTWGSR elsewhere[34] by the following Langmuir–Hinshelwood initial reaction rate

$$(-r_{CO})^0 = \frac{k\left(P_{CO}P_{H_2O} - \frac{P_{CO_2}P_{H_2}}{K_e}\right)}{(1 + K_{CO}P_{CO} + K_{H_2O}P_{H_2O} + K_{H_2}P_{H_2} + K_{CO_2}P_{CO_2})^2} \quad (2)$$

in which the kinetic and adsorption constants have been assumed to follow the Arrhenius and van't Hoff expressions, respectively, with the parameters as listed in Table 2.

Chlorine adsorption and deactivation

The feed stream entering the LTWGS reactor is assumed to be free of sulfur compounds. Moreover, the reaction temperature is kept at <503 K, ensuring that copper particles of the catalyst are far from being sintered. Based on these assumptions, deactivation of the catalyst is attributed exclusively to chlorine poisoning. It was assumed that the molar flow rate of chlorine was proportional to the total molar feed flow rate entering the reactor.

Taking into account the experimental data published in the literature,[15,33] a first order of chlorine partial pressure with respect to the chlorine adsorption on the catalyst active sites was assumed. Thus, the reaction rate of the chlorine adsorption can be described by the following kinetic equation

$$(-r_{Cl}) = k_{Cl}P_{Cl}a = k_{Cl}P^0_{Cl}(1 - X_{Cl})a \quad (3)$$

The assumption that catalyst deactivation is attributed exclusively to the chlorine irreversible adsorption on the active sites implies that the deactivation rate is also first order with respect to the chlorine partial pressure in the reactant mixture

$$-\frac{da}{dt} = -k_dP_{Cl}a = -k_dP^0_{Cl}(1 - X_{Cl})a \quad (4)$$

This assumption is realistic for a wide range of reaction conditions at which the catalyst deactivation takes place by chemisorption of poison molecules over the catalyst active centers in a one-to-one molar proportion.

Transformation of equations into discrete form

The catalyst bed has been divided into a series of N differential fixed-bed subreactors connected to each other. Considering N is large enough, each differential fixed-bed subreactor can be assumed as a perfectly mixed reactor, following the methodology proposed by González-Velasco et al.[24] Thus, the nth subreactor represents the n/N dimensionless position along the integral reactor. The time coordinate could also be divided into τ intervals.

After the spatiotemporal discretization, Eqs. 3 and 4 can be solved by the finite-differences approximation method, as follows

$$(-r_{Cl})(n,t) = \frac{X_{Cl}(n,t) - X_{Cl}(n-1,t)}{(\Delta W/F^0_{Cl})} = k_{Cl}P^0_{Cl}[1 - X_{Cl}(n,t)]a(n,t) \quad (5)$$

$$-\frac{da}{dt} = \frac{a(n,t) - a(n,t-1)}{\Delta t} = -k_dP^0_{Cl}[1 - X_{Cl}(n,t)]a(n,t) \quad (6)$$

Table 2. Values of the Frequency Factors and the Activation and Adsorption Energies for the Low-Temperature WGSR Rate Equation

Parameter	Frequency Factor	E_a or ΔH_a (kJ/mol)
k (mol g^{-1} h^{-1} Pa^{-2})	9.351×10^{-3}	57.47
K_{CO} (Pa^{-1})	1.737×10^{-6}	−11.35
K_{H_2O} (Pa^{-1})	4.668×10^{-7}	−14.90
K_{H_2} (Pa^{-1})	4.441×10^{-7}	−14.44
K_{CO_2} (Pa^{-1})	3.563×10^{-7}	−16.38

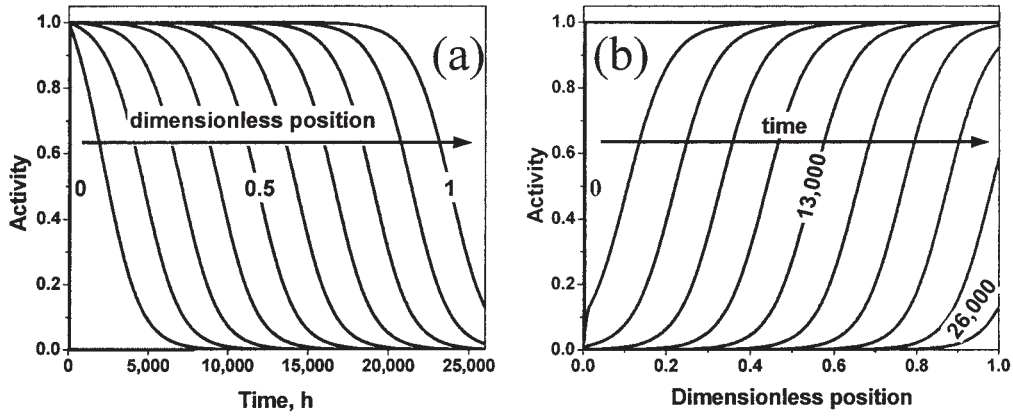

Figure 1. Activity–time and activity–dimensionless position profiles calculated for the base case.

where $a(n, 0) = 1$ and $X_{Cl}(0, t) = 0$ for $\forall n, t$.

Therefore, at any operation time t, the main reaction rate is

$$(-r_{CO}) = (-r_{CO})^0 a \tag{7}$$

which the finite-differences form gives

$$(-r_{CO})(n, t) = \frac{X_{CO}(n, t) - X_{CO}(n-1, t)}{(\Delta W/F^0_{CO})} = (-r_{CO})^0(n, t)a(n, t) \tag{8}$$

For the application of the Euler–Cauchy finite-differences method, ΔW and Δt were taken as the step sizes, resulting in the local errors $(\Delta W)^2$ and $(\Delta t)^2$.[35] For the discrete reactor model, $N = 100$ and $\tau = 1000$ were used, values that ensure good stability of the solved equation system with moderate computation time requisites. The differential Eqs. 5, 6, and 8 were solved by the finite-difference approximation method.

Energy balance

Because the LTWGSR is exothermic, and adiabatic operation conditions were assumed, the reactor energy balance must also be solved to determine the temperature variation along the catalyst bed. The energy balance solution for each node of the discrete grid is

$$T(n, t) = T^0(n, t) + J^*[X_{CO}(n, t) - X_{CO}(0, t)] \tag{9}$$

where $J^* = y^0_{CO}[-\Delta H_r/C_P]$ is the maximum adiabatic temperature rise along the reactor. Typically, a maximum value of 23.76 K for this parameter was obtained, assuming the mean values of 40.05 kJ/mol and 33.40 J mol^{-1} K^{-1} for $(-\Delta H_r)$ and C_P, respectively.

Activity profile

At given operating conditions, because the maximum temperature rise was less than 35 K, chlorine adsorption (k_{Cl}) and deactivation (k_d) reaction constants were assumed to be independent of temperature at their respective average values in the interval (2.112×10^{-6} mol g^{-1} h^{-1} Pa^{-1} and 1.974×10^{-7} h^{-1} Pa^{-1}, respectively).[33] This assumption simplifies the solution of chlorine mass balance and the deactivation equation. Consequently, the solution of the CO mass balance for changing temperature values is not necessary.

The activity vs. dimensionless position and activity vs. time of reaction profiles, obtained by the solution of Eqs. 5 and 6, are shown in Figures 1a and 1b, respectively. The shape of both calculated profiles confirmed the validity of the assumption that $(-r_{Cl})$ and $(-da/dt)$ are first order in chlorine partial pressure, presenting the same shape as that reported for industrial data.[15,33]

The Optimization Problem

A total operation time of 26,000 h was chosen (about 3 years), representing the lifetime of the industrial LTWGS catalyst. As a result of deactivation, during operation the reactor outlet CO conversion gradually decays with time; the operation time when CO outlet conversion falls to the lowest permissible value is called the *Catalyst Lifetime* (*CLT*). The production to be maximized is the molar amount of converted CO until the catalyst lifetime is consumed, called *Efficient Production* (*EP*)

$$EP = \int_0^{CLT} F^0_{CO} X_{CO} dt \tag{10}$$

Total Production (*TP*) is also defined by Eq. 10, extended to a total operation time, that is, changing the integral upper limit to 26,000 h. As a result of deactivation, during the last period of operation, the CO outlet conversion can fall below the lowest permissible value, taken as 0.85, consequently increasing CO concentration in the reactor outlet. Within this period, the CO removal by the WGSR is inefficient and further purification of hydrogen-rich gas is needed to increase the CO removal, thus increasing the operational costs.

Thus, CO conversion, chlorine conversion, and catalyst activity describe the system state variables, whereas the control variable of the system was the inlet temperature $T^0(t)$. The admission control region for the control variable has been defined as

$$U = \{T^0_{min} = 448 \text{ K} \le T^0(t) \le T^0_{max} = 503 \text{ K}\} \tag{11}$$

Table 3. Parameter Values, *EP* and *ER* for Constant and Time-Variable Optimum Inlet Temperatures

Case Study	Variation	Constant T^0 (K)	Constant *EP* (kmol CO)	Constant *ER* (GJ)	Elasticity (η)	Time-Variable α	β	γ ($\times 10^8$)	Time-Variable *EP* (kmol CO)	Time-Variable *ER* (GJ)
I	—	465	956.20	29.1	—	448	0	2.635	968.04	10.1
IIa	$1.05 \times \hat{F}^0$	481	980.30	59.3	0.69	448	0	4.493	1010.32	18.1
IIb	$0.95 \times \hat{F}^0$	455	917.50	11.4	0.43	448	0	1.290	922.41	4.7
IIIa	$1.15 \times \hat{G}^0$	465	963.60	30.8	0	448	0	2.587	975.81	11.0
IIIb	$0.85 \times \hat{G}^0$	466.5	943.25	29.9	−0.02	448	0	2.699	959.63	9.4
IVa	$1.30 \times \hat{P}$	461	961.70	22.2	−0.03	448	0	1.947	969.76	7.5
IVb	$0.70 \times \hat{P}$	472	948.22	41.1	−0.05	448	0	3.517	965.70	13.5
Va	$1.02 \times \hat{P}^0_{\mathrm{Cl}}$	470	949.78	37.6	0.54	448	0	3.237	966.36	9.6
Vb	$0.98 \times \hat{P}^0_{\mathrm{Cl}}$	456	966.40	13.7	0.97	448	0	2.095	969.44	6.2
VIa	$1.05 \times \hat{P}^0_{\mathrm{H_2}}$	470.5	930.40	38.7	0.24	448	0	3.103	953.12	11.9
VIb	$0.95 \times \hat{P}^0_{\mathrm{H_2}}$	461.5	962.10	23.1	0.15	448	0	2.172	970.96	8.4
VIIa	$0.95 \times \hat{P}^0_{\mathrm{CO}}$	464.5	1012.50	27.4	−0.02	448	0	2.476	1022.52	9.6
VIIb	$0.95 \times \hat{P}^0_{\mathrm{CO}}$	465.5	908.10	29.9	−0.02	448	0	2.795	917.18	10.7
VIIIa	$2.0 \times \hat{P}^0_{\mathrm{In}}$	464.5	925.40	28.2	∼0	448	0	2.677	934.13	10.3
VIIIb	$0.5 \times \hat{P}^0_{\mathrm{In}}$	465.5	967.40	29.9	∼0	448	0	2.600	976.95	10.0

A lower admissible limit for the feed inlet temperature of 448 K reflected the requirement to carry out the reaction in the gas phase. The minimum inlet temperature for the LTWGS reactor has been calculated at operating pressures as the dew temperature of the feed mixture. A safety margin—that is, a temperature 10 K higher than this minimum inlet temperature—has been used to avoid any accidental change of reaction conditions causing steam condensation within the reactor, then covering the catalyst pores. The upper value was established as 503 K to avoid sinterization of copper particles. The *EP* was obtained by integrating Eq. 10 according to the Simpson rule. The control variable was parameterized as a second-order polynomial function of time as follows

$$T^0(t) = \alpha + \beta t + \gamma t^2 \tag{12}$$

because this approach facilitates computation.[36-38] The search for the optimum parameters of inlet time-variable temperature has been carried out by constrained nonlinear minimization using the Levenberg–Marquardt algorithm using Matlab software (The MathWorks, Natick, MA).

Two optimization strategies have been used: (1) constant inlet temperature and (2) time-variable inlet temperature. Using the first strategy, *CLT*, *TP*, and *EP* were evaluated for different isothermal inlet temperatures. The isothermal inlet temperature that allows the highest *EP* is chosen as the optimum. The second strategy consisted in the calculation of the optimum inlet temperature time-trajectory for which the maximum *EP* was achieved.

The computation algorithm for optimization was as follows: (1) the initial parameter values were chosen for the inlet temperature in Eq. 12 (taking parameters β and γ as zero for the isothermal strategy); (2) catalyst activity was calculated for the discrete grid by simultaneous solution of Eqs. 5 and 6; (3) the carbon monoxide mass balance was solved for each node of the grid; (4) production was calculated by integrating the outlet conversion-time integral (Eq. 10); and (5) the procedure was repeated until the maximum production was achieved.

Energy requirements

The energy requirement for heating the LTWGS feed stream has been calculated. The HTWGS reactor effluent temperature is about 703 K. After its cooling by water addition to 448 K, the stream enters the LTWGS reactor. The energy requirement for heating the LTWGS reactor inlet flow was calculated according to

$$ER = F^0 \int_0^{CLT} \bar{C}_P[T^0(t) - \hat{T}]dt \tag{13}$$

where $\bar{C}_P$ is the mean specific heat of the feed mixture and $\hat{T}$ is the temperature from which the feed stream has to be heated (taken as 448 K).

Elasticity

The responsiveness of the optimum inlet temperature to process variables (Z) was used to compute sensitivity. *Elasticity* (η) can be defined as

$$\eta = \frac{\Delta T^0/T^0}{\Delta Z/Z^0} \tag{14}$$

Positive elasticity implies the process variable and optimum T^0 change in the same direction, whereas negative elasticity implies they change in the opposite direction. The higher the absolute value of elasticity, the higher the sensitivity of optimum T^0 with respect to the variable.

The operational variables were changed as ±5% in total inlet flow rate ($\hat{F}^0$), ±15% in steam-to-gas ratio ($\hat{G}^0$), ±30% in pressure ($\hat{P}^0$), ±2% in inlet chlorine content ($\hat{P}^0_{\mathrm{Cl}}$), ±5% in hydrogen content ($\hat{P}^0_{\mathrm{H_2}}$), ±5% in CO content ($\hat{P}^0_{\mathrm{CO}}$), and +100% and −50% in inert content ($\hat{P}^0_{\mathrm{In}}$).

Results and Discussion

Optimization of the base case (row I of Table 3)

For the reaction conditions listed in Table 1 (the base case) the optimum constant inlet temperature resulted in 465 K with an *EP* of 956.20 kmol CO converted during the *CLT* of 26,000 h (an equivalent outlet conversion of 0.942 in the whole operation time), as shown in Figure 2. When the lower inlet temperature was considered, a lower value of *EP* was observed

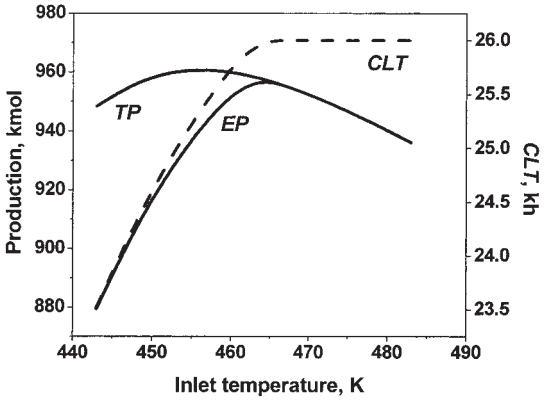

Figure 2. Total Production (*TP*), Efficient Production (*EP*), and Catalyst Lifetime (*CLT*) obtained for different constant inlet temperatures.

because of the shorter *CLT*, as shown in Figure 2. Note that a larger amount of converted CO moles could be obtained if the constant inlet temperature were 456.5 K, obtaining a *TP* of 961.0 kmol CO, although the *CLT* in these conditions would be of 25,203 h, thus requiring a premature catalyst change.

The outlet CO conversion trajectories for a set of constant inlet temperatures are depicted in Figure 3. In this graphical representation, the area below the curves corresponds to the *EP*. The crosslink of the outlet CO conversions for different isothermal inlet temperatures allows the existence of an optimal time-trajectory for an inlet temperature.

In the case of assuming second-order polynomial time-trajectory for the inlet temperature (Eq. 12), the following equation was deduced (broad line in Figure 3)

$$T^0(t) = 448 + 2.635 \times 10^{-8} \times t^2 \qquad (15)$$

An inlet temperature increase of 17.8 K and *EP* of 968.04 kmol CO for the *CLT* of 26,000 h was obtained (an equivalent outlet conversion of 0.954 in the whole operation time) with respect to the previous policy.

Thus, the optimum time-trajectory inlet temperature operation allows an energy saving over 26,000 h of operation of 19.0

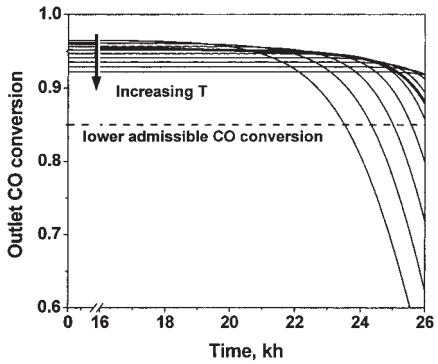

Figure 3. Reactor outlet CO conversion time-trajectory obtained for various constant inlet temperatures operating 26,000 h and the optimum time-trajectory inlet temperature (broad line).

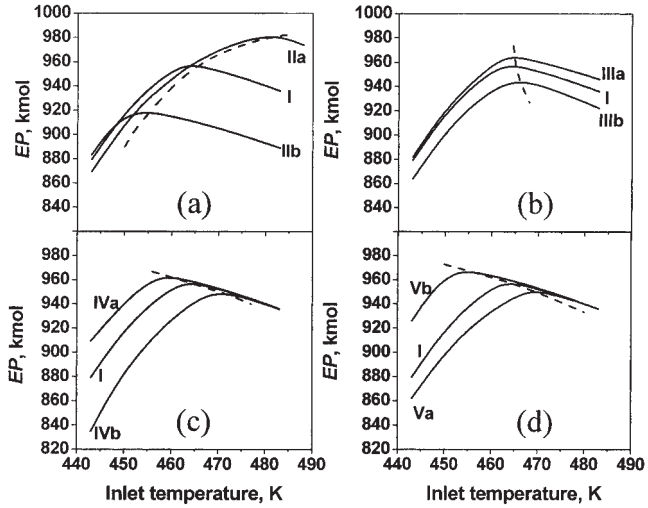

Figure 4. *EP* evolution for constant inlet temperature and optimum time-trajectory inlet temperatures for different case studies.

Variation of (a) inlet total flow rate, (b) steam-to-gas ratio, (c) pressure, and (d) inlet chlorine content. Letters a and b after roman number are for increase and decrease, respectively, of base case value of parameter.

GJ with respect to operating with optimal constant inlet temperature (that is, 65.3%). Row I of Table 3 summarizes the optimization results for the base case.

The curve representing the outlet CO conversion change with time is concave, as shown in Figure 3. This shape is based on two contradictory effects: as a result of the adiabatic operation conditions, the exothermicity causes an increase of temperature along the reactor, which enhances the kinetic rate constant that counterbalances the decrease in activity. Because the chemisorption of chlorine occurs gradually with the subsequent deactivation front, the fraction of the catalyst that was not affected by the poison remains highly active.

Sensitivity analysis with respect to process variables

The *EP* sensitivity as well as the optimum inlet temperature sensitivity were investigated with respect to the process variables such as inlet total flow rate, steam-to-gas ratio, pressure, chlorine concentration, hydrogen concentration, CO concentration, and inert concentration.

Total inlet flow rate, $\hat{F}^0$

Total inlet flow rate modification alters the contact time of the reactant mixture with the catalyst, and thus the space time for the main reaction as well as for the catalyst deactivation caused by chlorine adsorption. The value of the total inlet molar flow was varied by increasing or decreasing the nominal value by 5%.

Figure 4a shows the influence of the total inlet molar flow rate on the *EP* when the inlet temperature was maintained constant. The higher the F^0, the higher isothermal inlet temperature is necessary to achieve the maximum *EP*. The optimum inlet temperature seems to be very sensitive to the change of the inlet flow rate having $\eta = +0.56$. By increasing the nominal flow rate by 5% the optimum inlet temperature in-

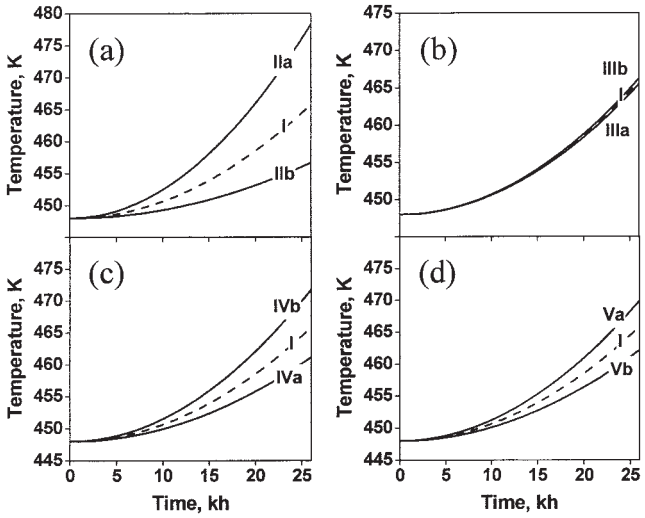

Figure 5. Optimum inlet time-trajectory evolution for variation of (a) inlet total flow rate, (b) steam-to-gas ratio, (c) pressure, and (d) inlet chlorine concentration.

Letters a and b after roman number are for increase and decrease, respectively, of base case value of parameter.

creased by 16 K, whereas when the flow rate was decreased by 5%, an inlet temperature drop of 10 K was calculated. The *EP* obtained resulted in 917.50 and 980.30 kmol CO for the lower and higher values of the parameter, respectively.

When the inlet temperature was varied with time, even higher *EP* could be achieved. Optimum inlet temperature time-trajectories for different total inlet flow rates are shown in Figure 5a. The total inlet flow increase is reflected by a steeper increase of the reactor inlet temperature compared to the nominal trajectory. If the value of $\hat{F}^0$ is increased by 5%, the inlet temperature just at the end of the *CLT* reaches 478.4 K, 12.6 K higher than the value obtained for the nominal F^0. On the other hand, an inlet flow rate decrease of 5% causes the temperature to be increased to 456.8 K, which is 9.1 K below the value obtained for nominal F^0. *ER* increases with F^0, but on the other hand, operating with time-varying inlet temperature supposes a mean energy saving of 64% with respect to the isothermal case. Rows IIa and IIb of Table 3 summarize the results of this optimization.

Steam-to-gas ratio, $\hat{G}^0$

The steam-to-gas ratio (G) is a very important operation parameter in WGSR. For the base case, $\hat{G}^0 = 0.61$ was given (Table 1). Steam, present in the reaction mixture, influences the reaction equilibrium toward higher CO conversion. On the other hand, an excess of steam dilutes the reaction mixture, thus diminishing the adiabatic temperature increase inside the reactor, as the J^* value is diminishing.

The sensitivity study was done varying $\hat{G}^0$ by $\pm 15\%$. *EP* evolution maintaining the constant inlet temperature is shown in Figure 4b. $\hat{G}^0$ does not modify the constant inlet temperature to achieve the maximum *EP*, given that for the three cases studied the optimum inlet temperatures lay within an interval of 1.5 K ($\eta = -0.02$). However, the *EP* obtained for the highest and lowest G^0 values differs substantially: 963.60 and 943.25 kmol CO, respectively. The similitude of temperatures can be explained as a consequence of two mutually antagonistic phenomena: the main reaction rate is favored by higher water content and, for this, higher temperatures are preferred because the deactivation rate is constant with temperature. On the other hand, the higher water contents avoid temperature increases in the reactor.

The optimum inlet temperature time-trajectory allows the reactor to operate with higher *EP* than that obtained for the constant inlet temperature, with a mean energy saving of 66%. Figure 5b shows the optimum inlet temperature time-trajectories for both case studies, compared with the base case. As in the case of constant inlet optimum temperatures the inlet temperature heating during the operation time is practically the same (a variation of about 0.8 K was evaluated). Rows IIIa and IIIb of Table 3 summarize these results.

Pressure, $\hat{P}^0$

A change of operation pressure modifies the partial pressures of reactants, and subsequently the WGSR rate, chlorine adsorption rate, and deactivation rate. The system pressure was modified within the range of $\pm 30\%$. Because 1723 MPa is the nominal value, a lower limit of 1216 MPa and an upper limit of 2230 MPa were established. The influence of pressure on *EP* is shown in Figures 4c and 5c for constant and time-variable inlet temperatures, respectively. Unlike the total inlet flow rate, the pressure increase has a negative effect on the optimum inlet temperature, having a $\eta = -0.04$. The influence of the operation pressure variation on *EP* is summarized in rows IVa and IVb of Table 3, for constant and time-varying inlet temperature strategies, respectively.

Inlet chlorine concentration, $\hat{P}^0_{Cl}$

The nominal value of poison concentration in the feed stream was considered to be 10^{-3} ppm, taken from Sen et al.,[39] and thus $P^0_{\mathrm{Cl}} = 6.383 \times 10^{-4}$ Pa was calculated. This value was varied within the range of $\pm 2\%$. Modification of this parameter is reflected in both the chlorine partial pressure and in its molar flow rate. Thus, the poison adsorption mass balance is not modified; however, the deactivation rate undergoes changes.

The optimization results are shown in Figures 4d and 5d and summarized in rows Va and Vb of Table 3. *EP* reaches its maximum values at 456 and 470 K for the lower and higher chlorine contents, respectively, when a constant inlet temperature is performed. The reduction of 2% in chlorine content supposes a 1.1% increase of *EP* with respect to the base case; on the other hand, an increase of 2% poison supposes a reduction of 0.7% in *EP* ($\eta = +0.75$). When the optimal inlet temperature time-trajectory is applied, the system with higher chlorine content must be heated faster than the system with lower chlorine content, which is 4.1 K higher and 3.6 K lower, respectively, than the base case at the end of the 26,000 h of operation.

Inlet hydrogen ($\hat{P}^0_{H_2}$)*, carbon monoxide* ($\hat{P}^0_{CO}$)*, and inert concentration* ($\hat{P}^0_{In}$)

The feed gas composition influences the optimum inlet temperature strategies. The feed stream composition entering the primary reformer unit could be as varied as natural gas, gas oil, naphtha, and even carbon. Therefore, the outlet gas stream

composition may also vary. To model this parameter, the stream hydrogen, carbon monoxide, and inert content was varied by ±5% (hydrogen), ±5% (CO), and +100 and −50% (inert content) from the nominal value.

EP change with constant inlet temperature is shown in Figure 6, whereas Figure 7 shows the optimum time-varying inlet temperature trajectory. The higher the inlet hydrogen content, the higher the constant optimum temperature, but the lower the maximum of *EP* ($\eta = +0.20$). The elasticity respect to CO and inert content is almost zero (−0.02 and +0.001, respectively), indicating that their modification does not substantially alter the optimum inlet temperatures. Optimization results are displayed in Table 3: rows VIa and VIb for hydrogen, rows VIIa and VIIb for CO, and rows VIIIa and VIIIb for inert content.

Conclusions

An industrial, adiabatic reactor for LTWGSR subject to catalyst deactivation by irreversible chlorine adsorption was modeled assuming a temperature-independent deactivation. The inlet temperature optimal policies were calculated to maximize the Efficient Production (*EP*) of the reactor. The finite-differences approximation method was used to compute the differential equations. The maximum value of *EP* was obtained for time-trajectory inlet temperature, about 1.24% higher than the reactor production for optimum constant inlet temperature conditions. Moreover, the use of time-trajectory policy for the inlet temperature resulted in a substantial decrease of energy consumed to heat the inlet stream for LTWGS reactor compared to that of the constant inlet temperature strategy (65.3%).

Furthermore, a sensitivity study was carried out modifying the operation variables. Elasticity of optimum inlet temperature is positive with respect to total inlet flow rate, the inlet chlorine content, and also the inlet hydrogen content; that is, the increase of the overall flow rate, chlorine content, or hydrogen content in the feed caused the shift of optimum isothermal inlet temperature as well as temperature increase during operation at time-dependent inlet temperature conditions to a higher value. On the other hand, the opposite situation was found for variation of steam-to-gas ratio, pressure, and CO content, whereas practically zero elasticity was found for inlet inert content. Elasticity with respect to steam-to-gas ratio is close to zero, resulting from its ambiguous effect of shifting the reaction equilibrium toward the reaction products, while simultaneously diluting the reaction mixture and buffering the adiabatic reaction temperature increase.

In all studied cases, the optimum time-trajectory control of the inlet temperature supposed important energy savings compared to that of the optimum isothermal inlet temperature operation of the LTWGS reaction.

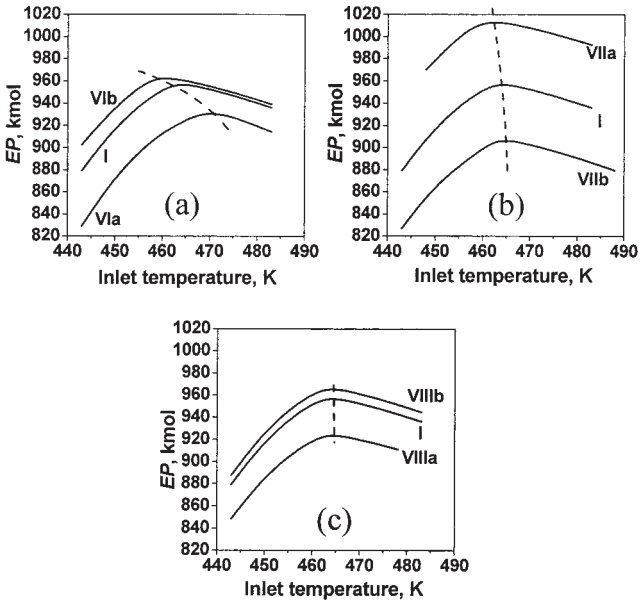

Figure 6. *EP* evolution for constant inlet temperature and optimum time-trajectory inlet temperatures for different case studies.

Variation of (a) inlet hydrogen content, (b) inlet CO content, and (c) inlet inert content. Letters a and b after roman number are for increase and decrease, respectively, of base case value of parameter.

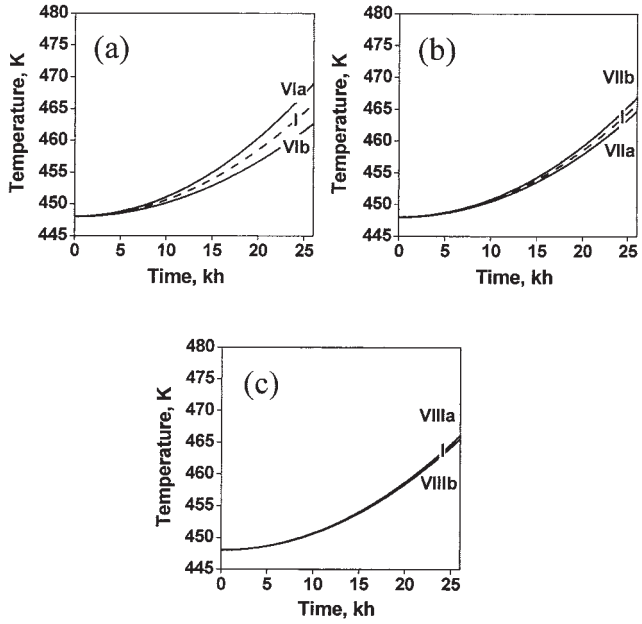

Figure 7. Optimum inlet time-trajectory evolution for variation of (a) inlet hydrogen concentration, (b) inlet CO concentration, and (c) inlet inert concentration.

Letters a and b after roman number are for increase and decrease, respectively, of base case value of parameter.

Notation

a = activity
C_P = specific heat, J mol^{-1} K^{-1}
CLT = catalyst lifetime, h
EP = efficient production, mol
ER = energetic requirement, J
F_j = molar flow rate of compound j, mol h^{-1}
G = steam-to-gas molar ratio
J^* = maximum adiabatic temperature rise, K
k = LTWGSR kinetic constant, mol g^{-1} h^{-1} Pa^{-2}
k_{Cl} = chlorine adsorption reaction kinetic constant, mol g^{-1} h^{-1} Pa^{-1}
k_d = deactivation rate kinetic constant, h^{-1} Pa^{-1}
K_j = adsorption constant for compound j in LTWGS reaction, Pa^{-1}
K_e = WGSR equilibrium constant

N = total number of subreactors
n = subreactor
P = pressure, Pa
P_j = partial pressure of compound j, Pa
$(-r_{CO})$ = WGSR rate, mol h^{-1} g^{-1}
$(-r_{Cl})$ = chlorine adsorption reaction rate, mol h^{-1} g^{-1}
t = time, h
T = temperature, K
TP = total production, mol
U = admissible region for the control variable
W = catalyst weight, g
X_j = conversion of compound j
y_j = mole fraction of compound j
Z = generic process variable

Greek letters

α, β, γ = parameters for time-variable inlet temperature
ΔH_r = WGSR heat, J mol^{-1}
τ = time intervals
η = elasticity

Subscripts

min = minimum
max = maximum

Superscripts

$\bar{}$ = mean value
0 = inlet, initial value
^ = nominal value

Literature Cited

1. Tanaka Y, Utaka T, Kikuchi R, Sasaki K, Eguchi K. Water gas shift reaction over Cu-based mixed oxides for CO removal from the reformed fuels. *Appl Catal A: Gen*. 2002;6395:1-9.
2. Zalc JM, Löffler DG. Fuel processing for PEM fuel cells: Transport and kinetic issues of system design. *J Power Sources*. 2002;111:58-64.
3. Chunshan S. Fuel processing for low-temperature and high-temperature fuel cells. Challenges and opportunities for sustainable development in the 21st century. *Catal Today*. 2002;77:17-49.
4. Newsome DS. The water–gas shift reaction. *Catal Rev Sci Eng*. 1980;21:275-318.
5. Hawker PN. Shift CO plus steam to H_2. *Hydrocarbon Process*. 1982; 61:183-187.
6. Ettouney HM, Shaban HI, Nayfeh LJ. Theoretical analysis of high and low temperature shift converters: Process and product development. *Chem Eng Res Des*. 1993;71:189-195.
7. Singh CPP, Saraf DN. Simulation of high-temperature water–gas shift reactors. *Ind Eng Chem Process Des Dev*. 1977;16:313-319.
8. Bohlbro H. The kinetics of the water gas conversion at atmospheric pressure. *Acta Chem Scand*. 1961;15:502-520.
9. Chinchen GC, Logan RH, Spencer MS. Water–gas shift reaction over an iron oxide/chromium oxide catalyst. III. *Kinet React Appl Catal*. 1984;12:97-103.
10. Ferretti OA, González JC, Laborde MA, Moreno N. Kinetic study of the water gas shift reaction at high temperatures. *Lat Am J Chem Eng Appl Chem*. 1986;16:75-83.
11. Gutmann WR, Johnson RE. *Low Temperature Shift Reactions Using Copper–Zinc Oxide Catalysts*. U.S. Patent Number 3 546 140; 1970.
12. Ghiotti G, Boccuzzi F. Chemical and physical properties of copper-based catalysts for CO shift reaction and methanol synthesis. *Catal Rev Sci Eng*. 1987;29:151-182.
13. Hadden RA, Lambert PJ, Ranson C. Relationship between the copper surface area and the activity of $CuO/ZnO/Al_2O_3$ water–gas shift catalysts. *Appl Catal A: Gen*. 1995;122:L1-L4.
14. Amadeo NE, Laborde MA. Low temperature water gas shift reaction: Catalyst, kinetics and reactor design and optimisation. *Trends Chem Eng*. 1996;3:159-183.
15. Young PW, Clark CB. Why shift catalysts de-activate. *Chem Eng Prog*. 1973;69:69-74.
16. Ray N, Roy SK, Ganguli NC, Sen SP. Factor affecting the activity and life of industrial low-temperature shift catalyst. *Technology* 1973;10: 216-219.
17. Ray N, Rastogi VK, Chhabra DS, Dutta S, Sen SP. Deactivation of low temperature shift catalyst. II. Poisoning by chloride. *J Res Inst Catal Hokkaido Univ* 1982;30:25-38.
18. Mertzsch N, Joedicke G, Wolf F, Renger P. The effect of chloride poisoning of the ternary cupric oxide-zinc oxide-aluminum oxide catalyst for low-temperature carbon monoxide conversion. *Chem Tech* (*Leipzig*). 1984;36:245-247.
19. Grant AW, Ranney JT, Campbell CT, Evans T, Thorton G. The influence of chlorine on the dispersion of Cu particles on Cu/ZnO(0001) model catalysts. *Catal Lett*. 2000;65:159-168.
20. Twigg MV, Spencer MS. Deactivation of supported copper metal catalysts for hydrogenation reactions. *Appl Catal A: Gen*. 2001;212: 161-174.
21. Lovik L, Hillestad M, Hertzberg T. Long term dynamic optimization of a catalytic reactor system. *Comput Chem Eng*. 1998;22:S707-S710.
22. Lovik I, Hillstad M, Hertzberg T. Sensitivity in optimisation of a reactor system with deactivating catalyst. *Comput-Aided Chem Eng*. 2000;8:517-522.
23. Ajinkya MB, Ray WH. The optimization of axially dispersed packed bed reactors experiencing catalyst decay. *Chem Eng Sci*.. 1973;28: 1719-1729.
24. González-Velasco JR, Gutiérrez-Ortiz MA, Gutiérrez-Ortiz JI, González-Marcos JA. Analysis of the lumped and distributed optimal temperature trajectories for packed bed reactors with concentration dependent catalysts reactivation. *Can J Chem Eng*. 1990;68:860-866.
25. Pommersheim JM, Chandra K. Optimal batch reactor temperature policy for reactions with concentration dependent catalyst decay. *AIChE J*. 1975;21:1029-1032.
26. Cuthrell JE, Biegler LT. Simultaneous optimisation and solution methods for batch reactor control profiles. *Comput Chem Eng*. 1989;13:49-62.
27. Grubecki I, Wojcik M. Comparison between isothermal and optimal temperature policy for batch reactor. *Chem Eng Sci*. 2000;55:5161-5163.
28. Sadana A. On optimum temperature operations in deactivating fixed-bed reactors. *Chem Eng Commun*. 1980;4:51-55.
29. Romero A, Gonzalez-Velasco JR, Bilbao J. Anales deq uímica. *Quím Fís Ing Quím Ser A*. 1981;77:253-258.
30. Hong JC, Lee HH. Stepwise temperature set-point optimisation for isothermal fixed-bed reactor subject to catalyst deactivation. *J Chin Inst Chem Eng*. 1990;21:21-26.
31. Barreto GF, Ferretti OA, Farina IH, Lemcoff NO. Optimization of the operating conditions of CO converters. *Ind Eng Chem Process Des Dev*. 1981;20:594-603.
32. Faqir NM, Attarakih MM. Optimal temperature policy for immobilized enzyme packed bed reactor performing reversible Michaelis–Menten kinetics using the disjoint policy. *Biotechnol Bioeng*. 2002; 77:163-173.
33. González-Velasco JR, Gutiérrez-Ortiz MA, González-Marcos JA, Amadeo N, Laborde MA, Paz M. Optimal inlet temperature trajectories for adiabatic packed reactors with catalyst decay. *Chem Eng Sci*. 1992;47:1495-1501.
34. Ayastuy JL. *Conversión de Monóxido de Carbono a baja temperatura: Cinética del Proceso y Optimación de la operación industrial* PhD Thesis. Bilbao, Spain: Universidad del País Vasco/EHU; 2002.
35. Rosen O, Luss R. Evaluation of gradients for piecewise constant optimal control. *Comput Chem Eng*. 1991;15:273-281.
36. Hicks GA, Ray WH. Approximation methods for optimal control synthesis. *Can J Chem Eng*. 1971;49:522-528.
37. Buzzi-Ferraris G, Facchi E, Forzatti P, Tronconi E. Control optimization of tubular catalytic reactors with catalyst decay. *Ind Eng Chem Process Des Dev*. 1984;23:126-131.
38. González-Velasco JR, Gutiérrez-Ortiz MA, Romero-Salvador A. Optimization by lumped control of reactors with Langmuir–Hinshelwood catalyst deactivation. *Can J Chem Eng*. 1985;63:314-321.
39. Sen B, Ray N, Bhattachariya NB. Shift reaction on iron-chromia and copper based catalysts. *Chem Age India*. 1981;32:321-331.

Manuscript received Feb. 24, 2004, and revision received Nov. 4, 2004.